

Limits on an additional Z boson from e^+e^- annihilation data

K. Hagiwara

KEK, Tsukuba 305, Japan

and Department of Physics, University of Durham, Durham DH1 3LE, England

R. Najima

Yokohama College of Commerce, Yokohama 230, Japan

M. Sakuda

KEK, Tsukuba 305, Japan

N. Terunuma

Department of Physics, Hiroshima University, Hiroshima 730, Japan

(Received 14 August 1989)

We study the possibilities of an extra Z boson expected from E_6 grand unified theories by using the most recent e^+e^- annihilation data up to $\sqrt{s} = 57$ GeV. Limits on the mass and mixing angle for the extra Z boson are discussed. We find that the data fit well for an extra Z boson whose mass is in the range 100–400 GeV and which has an appreciable vector coupling to charged leptons and down-type quarks. The upper mass bound is marginal such that it disappears at the 2σ level even for the most favorable model (Z_χ).

I. INTRODUCTION

Although the standard $SU(2)_L \times U(1)_Y$ electroweak model¹ is in excellent agreement with low-energy phenomena^{2,3} and the properties of W and Z bosons,⁴ other models with one or more additional gauge bosons are not necessarily ruled out. Recently, several authors^{5,6,2,3} investigated the constraints on extra Z bosons from the existing low-energy neutral-current (NC) data and the observed W and Z masses. They gave constraints on the mass and mixing angle for the extra Z bosons expected in E_6 grand unified theory. Their lower limits are typically around 100–300 GeV (90% C.L.).

From the e^+e^- pair production rate at the CERN $p\bar{p}$ collider, the UA1 and UA2 Collaborations have set limits on the mass and the coupling strength of an extra Z boson, whose couplings to quarks and leptons, except for the global coupling strength, are assumed to be the same as those of the standard Z boson.⁷ Their lower limits are 180 GeV (UA2) and 173 GeV (UA1) at the 90% C.L. when the global coupling strength is set equal to that of the standard Z boson.

Of all the NC data, the energy scale of the interaction is largest in e^+e^- annihilation especially when KEK TRISTAN data are incorporated. At TRISTAN energies, the effect of the Z resonance is significant in the R measurements and the electroweak interference effect is clearly visible in the forward-backward asymmetry of the process $e^+e^- \rightarrow \mu^+\mu^-$ and $\tau^+\tau^-$. Recently, the AMY Collaboration⁸ as well as other TRISTAN experiments⁹ fitted the prediction of the standard model to all available R data and reported a somewhat lower value for M_Z than those from direct measurements.⁴

The aim of this paper is to reexamine the possibilities

of extra Z bosons expected from the E_6 grand unified theories in view of the most recent e^+e^- annihilation data published up to $\sqrt{s} = 57$ GeV. We find that the data have a tendency to give a slightly higher rate for $e^+e^- \rightarrow \text{hadrons}$ (R) whereas a slightly lower rate for $e^+e^- \rightarrow l^+l^-$ (R_{ll} for $l = \mu, \tau$) as compared to the standard-model predictions. Although neither of the above effects alone are very significant, these data are well accommodated by introducing an extra Z boson of mass in the range 100–400 GeV with appreciable vector couplings to charged leptons and down-type quarks.

II. THE MODEL WITH AN ADDITIONAL Z BOSON

The NC Lagrangian is denoted by

$$-L_{\text{NC}} = e(J_{\text{EM}}^\mu A_\mu + J_1^\mu Z_{1\mu}^0 + J_2^\mu Z_{2\mu}^0), \quad (1)$$

where A and Z_1^0 are the conventional photon and Z fields of the standard $SU(2)_L \times U(1)_Y$ model and Z_2^0 is the new neutral gauge boson associated with the extra $U(1)$ symmetry. J_{EM}^μ is the electromagnetic current and

$$J_\alpha^\mu = \sum_i \bar{\psi}_i \gamma^\mu (g_{\alpha L}^{0i} P_L + g_{\alpha R}^{0i} P_R) \psi_i, \quad (2)$$

for $\alpha = 1, 2$ are the neutral currents associated with Z_1^0 and Z_2^0 , respectively. The sum is taken over leptons and quarks, and $P_{L,R} = (1 \mp \gamma_5)/2$ are the left- and right-handed chirality projection operators. The physical mass eigenstates (Z_1, Z_2) are related to the above current eigenstates (Z_1^0, Z_2^0) as

$$\begin{aligned} Z_1 &= Z_1^0 \cos\theta_E + Z_2^0 \sin\theta_E, \\ Z_2 &= -Z_1^0 \sin\theta_E + Z_2^0 \cos\theta_E, \end{aligned} \quad (3)$$

TABLE I. The extra $U(1)_\beta$ charges of particles in the 27 of the E_6 grand unified theories.

Left-handed state	Charge
u, d, u^c, e^c	$Y_1 = \frac{1}{3}(\sqrt{5/8} \cos\beta + \sqrt{3/8} \sin\beta)$
d^c, ν_e, e	$Y_2 = \frac{1}{3}(\sqrt{5/8} \cos\beta - 3\sqrt{3/8} \sin\beta)$
ν^c	$Y_3 = \frac{1}{3}(\sqrt{5/8} \cos\beta + 5\sqrt{3/8} \sin\beta)$
D, H^+, H^0	$Y_H = -\frac{2}{3}(\sqrt{5/8} \cos\beta + \sqrt{3/8} \sin\beta)$
$D^c, \bar{H}^0, \bar{H}^-$	$Y_{\bar{H}} = -\frac{2}{3}(\sqrt{5/8} \cos\beta - \sqrt{3/8} \sin\beta)$
N	$Y_N = \frac{4}{3}\sqrt{5/8} \cos\beta$

where θ_E is the new mixing angle. The mass-squared matrix for the two gauge bosons (Z_1, Z_2) with masses (M_1, M_2) are given in the above two bases as

$$(Z_1 \ Z_2) \begin{pmatrix} M_1^2 & 0 \\ 0 & M_2^2 \end{pmatrix} \begin{pmatrix} Z_1 \\ Z_2 \end{pmatrix} = M_0^2 (Z_1^0 \ Z_2^0) \begin{pmatrix} 1 & b \\ b & a \end{pmatrix} \begin{pmatrix} Z_1^0 \\ Z_2^0 \end{pmatrix}, \quad (4)$$

where M_0 would be the Z_1^0 mass in the case of no mixing and is related to the W mass and the weak mixing angle as

$$M_0 = M_W / \cos\theta_W. \quad (5)$$

The mixing angle θ_E is given by

$$\tan^2\theta_E = \frac{M_0^2 - M_1^2}{M_2^2 - M_0^2} \quad (6)$$

and the model-dependent constants (a, b) can be expressed in terms of M_0, θ_E and the physical masses M_1 and M_2 as

$$a = \frac{M_1^2 + M_2^2 - M_0^2}{M_0^2}, \quad b = -\tan\theta_E \frac{M_2^2 - M_0^2}{M_0^2}. \quad (7)$$

In superstring-inspired models,¹⁰ the off-diagonal mass-squared matrix element b is induced by the vacuum expectation values (VEV's) v and \bar{v} of the two Higgs fields:

$$b = -2\lambda \sin\theta_W \frac{Y_H v^2 - Y_{\bar{H}} \bar{v}^2}{v^2 + \bar{v}^2}, \quad (8)$$

where λ denotes the relative strength of the extra $U(1)$ coupling g_E normalized to the standard $U(1)_Y$ coupling, $g_Y = e / \cos\theta$, and Y_H and $Y_{\bar{H}}$ are the extra $U(1)$ charges of the Higgs fields $H = (H^+, H^0)$ and $\bar{H} = (\bar{H}^0, \bar{H}^-)$, respectively. Requiring v^2 and $\bar{v}^2 \geq 0$ in Eq. (8), one obtains the inequality ("Higgs constraint"¹¹)

$$\begin{aligned} \text{Min}\{-Y_H, Y_{\bar{H}}\} &\leq -\frac{\tan\theta_E}{2\lambda \sin\theta_W} (M_2^2 / M_0^2 - 1) \\ &\leq \text{Max}\{-Y_H, Y_{\bar{H}}\}. \end{aligned} \quad (9)$$

The extra $U(1)$ generator Y_β in the E_6 grand unification models with the breakdown $E_6 \rightarrow G \times U(1)_\beta$, where G contains the standard-model group $SU(3) \times SU(2) \times U(1)_Y$, can be parametrized conveniently as

$$Y_\beta = Y_\psi \cos\beta + Y_\chi \sin\beta. \quad (10)$$

Here, the generators Y_ψ and Y_χ are associated with the $U(1)$ groups in the breakdown $E_6 \rightarrow SO(10) \times U(1)_\psi$ and $SO(10) \rightarrow SU(5) \times U(1)_\chi$. In the E_6 model, each family of fermions is classified in a 27 representation. Their extra $U(1)$ charges are listed in Table I (Ref. 12).

In general, the angle β may take arbitrary values in the E_6 grand unified theories. Angles $\beta=0, \pi/2, \arctan\sqrt{3/5}$ and $\arctan(-\sqrt{1/15})$ correspond to the charges for Z_ψ, Z_χ, Z_η , and Z_ν , respectively.¹³ Here, Z_η is found in superstring models¹⁴ where E_6 is broken directly to a rank-5 group. Another interesting model¹⁵ is Z_ν (model C of Ref. 3) with $\beta = \arctan(-\sqrt{1/15})$, where right-handed neutrinos (ν^c in Table I) are chargeless and hence allow for the "seesaw" solution¹⁶ of the neutrino mass problem.

In Table II we present the current basis coupling g_{2i}^{0f} ($i=L, R$) in terms of the charges listed in Table I. The normalization factor $\lambda = g_E / g_Y$ is expected to be unity when the underlying group breaks directly into $SU(3) \times SU(2) \times U(1)_Y \times U(1)_E$. If the breaking into $U(1)_Y$ occurs at energies lower than the energy where the splitting of the extra $U(1)_E$ takes place, $\lambda < 1$ is expected in general. In the following, we set $\lambda=1$ throughout the analysis and note² that the limits on M_2 and θ_E scale roughly as λ and $1/\lambda$, respectively.

III. e^+e^- ANNIHILATION CROSS SECTIONS

The lowest-order differential cross section for $e^+e^- \rightarrow f\bar{f}$ ($f=\mu, \tau, c$) including γ, Z_1 , and the extra Z_2 boson exchanges is given by

$$\begin{aligned} \frac{d\sigma}{d\cos\theta} &= \frac{\pi\alpha^2}{8s} [(1 + \cos\theta)^2 (|A_{LL}^{ef}|^2 + |A_{RR}^{ef}|^2) \\ &\quad + (1 - \cos\theta)^2 (|A_{LR}^{ef}|^2 + |A_{RL}^{ef}|^2)], \end{aligned} \quad (11)$$

with

$$A_{ij}^{ef} = Q_e Q_f + g_{1i}^e g_{1j}^f / s_{Z_1} + g_{2i}^e g_{2j}^f / s_{Z_2}$$

for $i, j=L, R$ and $s_{Z_\alpha} = s - M_{Z_\alpha}^2 + iM_{Z_\alpha} \Gamma_{Z_\alpha}$ for $\alpha=1, 2$.

TABLE II. Coupling strength of fermions to the extra gauge boson Z_β . Y_1, Y_2 , and Y_3 are given in Table I.

	ν_e	e	u	d
g_{2L}^{0f}	$\lambda Y_2 / \cos\theta_W$	$\lambda Y_2 / \cos\theta_W$	$\lambda Y_1 / \cos\theta_W$	$\lambda Y_1 / \cos\theta_W$
g_{2R}^{0f}	$-\lambda Y_3 / \cos\theta_W$	$-\lambda Y_1 / \cos\theta_W$	$-\lambda Y_1 / \cos\theta_W$	$-\lambda Y_2 / \cos\theta_W$

Q_f is the electric charge of f normalized to the proton charge e . $g_{\alpha L}^f$ ($\alpha=1,2$) is the left-handed coupling to the mass eigenstates Z_α , also normalized to the unit charge e , and is expressed in terms of the couplings in the current basis $g_{\alpha L}^{0f}$ ($\alpha=1,2$) of Eq. (2) as

$$\begin{aligned} g_{1L}^f &= g_{1L}^{0f} \cos\theta_E + g_{2L}^{0f} \sin\theta_E, \\ g_{2L}^f &= -g_{1L}^{0f} \sin\theta_E + g_{2L}^{0f} \cos\theta_E, \end{aligned} \quad (12)$$

according to the Z_1^0 - Z_2^0 mixing (3). The relations between $g_{\alpha R}^f$ and $g_{\alpha R}^{0f}$ are obtained from Eq. (12) by simply replacing the subscripts L by R . The standard-model couplings to Z_1^0 are given as

$$g_{1L}^{0f} = (I_3 - \sin^2\theta_W Q_f) / (\sin\theta_W \cos\theta_W)$$

and $g_{1R}^{0f} = -\tan\theta_W Q_f$, where I_3 denotes the third component of the weak isospin. The imaginary parts of the inverse propagators, $M_{Z_\alpha} \Gamma_{Z_\alpha}$, are irrelevant up to TRISTAN energies and hence they are set to zero in the present analysis.

The leptonic production cross sections $R_{\mu\mu}, R_{\tau\tau}$ and the forward-backward asymmetries $A_{\mu\mu}, A_{\tau\tau}$, and A_{cc} can be easily calculated from Eq. (11), where fermion-mass effects and QCD corrections for A_{cc} are negligible.¹⁷ The hadronic R ratio including quark-mass effects and QCD effects is expressed in terms of the amplitudes A_{ij}^{eq} of Eq. (11) as

$$\begin{aligned} R &= 3 \sum_q \left[\frac{1}{2} \beta_q (3 - \beta_q^2) R_{\nu\nu}^q (1 + C_{\text{QCD}}^V) \right. \\ &\quad \left. + \beta_q^3 R_{AA}^q (1 + C_{\text{QCD}}^A) \right], \end{aligned} \quad (13)$$

with

$$\begin{aligned} R_{\nu\nu}^q &= \frac{1}{8} (|A_{LL}^{\text{eq}} + A_{LR}^{\text{eq}}|^2 + |A_{RL}^{\text{eq}} + A_{RR}^{\text{eq}}|^2), \\ R_{AA}^q &= \frac{1}{8} (|A_{LL}^{\text{eq}} - A_{LR}^{\text{eq}}|^2 + |A_{RL}^{\text{eq}} - A_{RR}^{\text{eq}}|^2). \end{aligned} \quad (14)$$

Here, the QCD correction factors $C_{\text{QCD}}^{V(A)}$ are given^{18,19} by

$$C_{\text{QCD}}^{V(A)} = f_1^{V(A)} (\alpha_s/\pi) + f_2^{V(A)} (\alpha_s/\pi)^2 + f_3^{V(A)} (\alpha_s/\pi)^3, \quad (15)$$

with

$$\begin{aligned} f_1^V &= \frac{4\pi}{3} \left[\frac{\pi}{2\beta_q} - \frac{3+\beta_q}{4} \left[\frac{\pi}{2} - \frac{3}{4\pi} \right] \right], \\ f_1^A &= \frac{4\pi}{3} \left[\frac{\pi}{2\beta_q} - \left[\frac{19}{10} - \frac{22}{5}\beta_q + \frac{7}{2}\beta_q^2 \right] \left[\frac{\pi}{2} - \frac{3}{4\pi} \right] \right], \\ f_2^{V(A)} &= 1.986 - 0.115 N_f, \end{aligned} \quad (16)$$

$$f_3^{V(A)} = 70.985 - 1.2 N_f - 0.005 N_f^2 - 1.679 \frac{\left[\sum Q_q \right]^2}{3 \sum Q_q^2}.$$

Here, β_q is the velocity of the quark and $N_f=5$ is the number of quark flavors.

The strong coupling constant $\alpha_s(s)$ is defined in three-loop order as^{20,19}

$$\begin{aligned} b_0 \ln \left[\frac{s}{\Lambda_{\text{MS}}^2} \right] &= \frac{1}{a} + \frac{c_1}{2} \ln \frac{b_0^2 a^2}{1 + c_1 a + c_2 a^2} \\ &\quad + \frac{2c_2 - c_1^2}{\Delta} \left[\arctan \left[\frac{c_1 + 2c_2 a}{\Delta} \right] \right. \\ &\quad \left. - \arctan \left[\frac{c_1}{\Delta} \right] \right], \end{aligned} \quad (17)$$

with $\Delta = (4c_2 - c_1^2)^{1/2}$ and $a = \alpha_s(s)/\pi$. The coefficients are $b_0 = 1.917$, $c_1 = 1.261$, $c_2 = 1.475$ for $N_f = 5$. Here, $\Lambda_{\text{MS}} (= \Lambda_{\text{MS}}^{(\bar{s})})$ is the QCD scale parameter of the modified minimal-subtraction scheme^{21,20} in the effective five-flavor theory.²² This implicit equation for $\alpha_s(s)$ is easily solved numerically by iteration.

IV. DATA AND THE STANDARD-MODEL FIT

The χ^2 analysis is based on the total of 220 data points. They consist of total cross sections of $e^+e^- \rightarrow \mu^+\mu^-, \tau^+\tau^-$ ($R_{\mu\mu}, R_{\tau\tau}$) (Ref. 23) and those of hadrons (R) (Ref. 24), as well as the forward-backward charge asymmetries for reactions $e^+e^- \rightarrow \mu^+\mu^-, \tau^+\tau^-$ ($A_{\mu\mu}, A_{\tau\tau}$) (Ref. 23) and that of $c\bar{c}$ (A_{cc}) (Ref. 25) over the energy region $\sqrt{s} = 14-57$ GeV.

Statistical errors and systematic errors are added in quadrature. The overall normalization errors in $R_{\mu\mu}, R_{\tau\tau}$, and R measurements, due mainly to the uncertainty in the luminosity determination, are taken into account properly whenever they are given in the papers. All data from the SLAC and DESY e^+e^- colliders PEP and PETRA are corrected for initial-state radiation effects.²⁶ All the lepton data from TRISTAN are corrected for full electroweak effects.²⁷ For the treatment of R values from TRISTAN experiments, we followed the paper by the AMY Collaboration,⁸ which used the program including the full electroweak effects.²⁸ All these radiative corrections depend on the assumed values of the standard-model parameters, e.g., on M_Z and $\sin^2\theta_W$ values. We note, however, that as far as the deviations from the standard-model predictions are small, which is indeed the case in our analysis, we can directly confront our modified Born-cross-section formulas (11) and (13) with those radiatively corrected data.

First, we make the standard-model fit to the above data sample. In order to examine various aspects of the e^+e^- data, we have made fits separately to the following subsets of the data: (a) lepton only with 143 data points (R_{ll} and A_{ll} , $l = \mu, \tau$), (b) R only with 73 data points, and (c) all data ($R_{ll}, A_{ll}, R, A_{cc}$) with 220 data points.

The standard model has two parameters to be fitted, which we choose to be $\sin^2\theta_W$ and M_Z . For the R data, Λ_{MS} can also be regarded as an extra parameter. We have performed three different fitting procedures: (i) allowing all three parameters to be fitted by the e^+e^- data, (ii) constraining Λ_{MS} in a range measured by other experiments but allowing $\sin^2\theta_W$ and M_Z to be fitted by the data, and (iii) to fit only M_Z from the data by constraining both Λ_{MS} and $\sin^2\theta_W$ by other experiments.

We encountered a difficulty in the first procedure since the R data gave a correlation between $\sin^2\theta_W$ and $\Lambda_{\overline{\text{MS}}}$. Data prefer larger $\Lambda_{\overline{\text{MS}}}$ for smaller $\sin^2\theta_W$, e.g., for $\sin^2\theta_W=0.24, 0.23,$ and 0.22 we find $\Lambda_{\overline{\text{MS}}}=0.22, 0.26,$ and 0.31 GeV, respectively. This correlation occurs since at intermediate PETRA energies there appears a partial cancellation between destructive interference effects proportional to the electron vector coupling factor $(1-4\sin^2\theta_W)$ and the positive QCD correction. Because of this correlation, it is difficult to measure the electroweak parameters and $\Lambda_{\overline{\text{MS}}}$ simultaneously.

The QCD parameter is measured best at recent deep-inelastic scattering experiments,^{29,30} which found $\Lambda_{\overline{\text{MS}}}^{(4)}=0.238\pm 0.043$ GeV, where $\Lambda_{\overline{\text{MS}}}^{(4)}$ is the QCD scale parameter for four quark flavors. Using the matching condition between $\Lambda_{\overline{\text{MS}}}^{(4)}$ and $\Lambda_{\overline{\text{MS}}}^{(5)}$ (Refs. 22 and 31), we obtain³²

$$\Lambda_{\overline{\text{MS}}} = \Lambda_{\overline{\text{MS}}}^{(5)} = 0.15 \pm 0.03 \text{ GeV}, \quad (18)$$

for $m_b = 5$ GeV. Our results are insensitive to the variation of $\Lambda_{\overline{\text{MS}}}$ in the above range, and hence in the following we set $\Lambda_{\overline{\text{MS}}} = 0.15$ GeV as our standard value. The results of our fit with $\Lambda_{\overline{\text{MS}}} = 0.12$ or 0.18 GeV are reported when relevant.

When we constrain $\sin^2\theta_W$ from other experiments, we allow it to vary in the range^{2,3,30}

$$\sin^2\theta_W = 0.229 \pm 0.006. \quad (19)$$

Since $\Lambda_{\overline{\text{MS}}}$ is fixed to 0.15 GeV, the results are given only for the above two fitting procedures (ii) and (iii), and are summarized in Table III. When $\sin^2\theta_W$ is constrained, the errors include the uncertainty coming from varying $\sin^2\theta_W$ in the range (19). The experimental errors may have been estimated conservatively, as the values for χ^2/N_{DF} are much less than 1.0. As already reported by TRISTAN experiments,^{8,9} the fitted value for M_Z is somewhat lower than the values reported by the UA1 and UA2 Collaborations. We further note here the following points. R_{ll} is sensitive to the destructive interference between the γ - and Z -exchange amplitudes which are proportional to $(1-4\sin^2\theta_W)^2$, whereas A_{ll} measures the factor $1/(M_Z^2\sin^2\theta_W\cos^2\theta_W)$. The small

$\sin^2\theta_W$ and large M_Z solution of our unconstrained fit to leptonic data (see Table III) reflects the tendency that the observed R_{ll} is smaller than the standard-model prediction while the magnitude of A_{ll} is roughly in the expected range.

At $\Lambda_{\overline{\text{MS}}} = 0.12$ (0.18) GeV, our unconstrained fit to R data alone gives $\sin^2\theta_W = 0.232^{+0.03}_{-0.02}$ ($\sin^2\theta_W = 0.226^{+0.03}_{-0.02}$) and $M_Z = 87.5^{+2.2}_{-1.7}$ ($M_Z = 87.6^{+2.2}_{-1.7}$) GeV with $\chi^2_{\text{min}}/N_{\text{DF}} = 55.9/71$ ($55.4/71$). The difference is negligible.

V. LIMITS ON ADDITIONAL Z BOSONS

We now discuss the extra U(1) models of the E_6 grand unified theory, which are parametrized by the angle β . Since we fix the global coupling strength to be $\lambda=1$ ($g_E=g_Y$) and all the couplings are specified by the angle β (see Tables I and II), we have two additional parameters (M_2, θ_E) to be fitted by the data for each model.

For the standard-model parameters, we fix $\Lambda_{\overline{\text{MS}}} = 0.15$ GeV and allow $(M_0 = M_Z, \sin^2\theta_W)$ to vary. In principle, the constraint (19) from the low-energy measurements should be modified by the introduction of extra Z bosons. However, this variation of the fitted value of $\sin^2\theta_W$ has been found to be rather small for extra Z model parameters which are consistent with the low-energy data.³ In view of this observation, we study three fixed values of $\sin^2\theta_W$ in the range of (19), $\sin^2\theta_W = 0.223, 0.229,$ and 0.235 , to examine the sensitivity of our results to this parameter. For each $\sin^2\theta_W$ value, M_0 is allowed to vary.

The model predictions are then fitted to the e^+e^- data as well as the measured W and Z ($=Z_1$) masses^{4,30}:

$$M_W = 80.9 \pm 1.4 \text{ GeV}/c^2, \quad (20a)$$

$$M_{Z_1} = 91.9 \pm 1.8 \text{ GeV}/c^2. \quad (20b)$$

We consider only those models which satisfy the condition (5). $M_0\cos\theta_W$ is then constrained directly by the M_W data (20a). M_{Z_1} is calculated from the three parameters (M_0, M_2, θ_E) according to Eq. (6). Since the above two data of (20) are added, our χ^2 analysis consists of 222 data points with three parameters, $M_0, M_2,$ and θ_E for each fixed value of $\sin^2\theta_W$.

TABLE III. Summary of fits within the standard model. The results are given for two fitting procedures; (a) $\sin^2\theta_W$ and M_Z are allowed to vary and (b) only M_Z is fitted from the data by constraining $\sin^2\theta_W$ in the range 0.229 ± 0.006 . Errors given in the table correspond to $\Delta\chi^2 = \chi^2 - \chi^2_{\text{min}} = 1.0$.

	Lepton data	R data	All data
Unconstrained fit			
$\sin^2\theta_W$	$0.16^{+0.03}_{-0.02}$	$0.23^{+0.03}_{-0.02}$	0.24 ± 0.02
M_Z (GeV)	100 ± 6	$87.5^{+2.1}_{-1.7}$	$89.1^{+2.0}_{-1.9}$
$\chi^2_{\text{min}}/N_{\text{DF}}$	$89.5/141$	$55.6/71$	$148.7/218$
Constrained fit			
$\sin^2\theta_W$	0.229 ± 0.006	0.229 ± 0.006	0.229 ± 0.006
M_Z (GeV)	$90.0^{+1.9}_{-1.8}$	$87.5^{+2.0}_{-1.7}$	$89.0^{+1.4}_{-1.3}$
$\chi^2_{\text{min}}/N_{\text{DF}}$	$92.2/142$	$55.6/72$	$148.9/219$

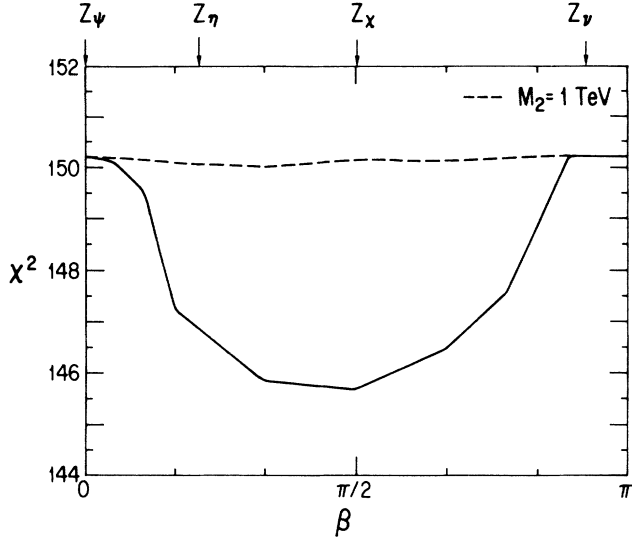


FIG. 1. The χ^2_{\min} of the fit for Z_β models are shown in solid line. The dashed line shows the χ^2 values when M_2 is fixed to 1 TeV while θ_E is allowed to vary. The curves are not smooth since only discrete sets of the Z_β models are examined and then linearly interpolated.

First, we show in Fig. 1 the χ^2_{\min} of the fit for Z_β boson as a function of the angle β . The χ^2 values are also plotted when M_2 is fixed to 1 TeV while θ_E is allowed to vary. Comparing χ^2 at $M_2=1$ TeV with χ^2_{\min} , one can easily calculate the confidence level of finite M_β values. It can be seen that the fit is best at $\beta \sim \pi/2$ and worst at $\beta=0, \pi$. The χ^2 value ($=153.4$) for the standard-model fit with $\sin^2\theta_W=0.229$ and $M_Z=91.9$ GeV should be equal to the χ^2 value for the extra U(1) model fit with $M_2=+\infty$ and $\theta_E=0$, and it is about $\Delta\chi^2=7.5$ above the minimum of the fit for Z_β boson with $\beta \sim \pi/2$. We repeated the analysis at two other $\sin^2\theta_W$ values, 0.223 and 0.235, and found that the location ($\beta \sim \pi/2$) and the depth of this dip are almost unaffected.

This feature of the fit is qualitatively understood as follows. One can easily confirm from Table II that the vector coupling of charged leptons (e, μ, τ) and down-type quarks to Z_β is proportional to $\pm\sin\beta$, whose magnitude is largest at $\beta=\pi/2$ (Z_χ) and zero at $\beta=0, \pi$ (Z_ψ). The vector coupling of up-type quarks to Z_β is always zero. In the total rates R_{ll} and R , only the vector coupling part of the extra Z-exchange amplitudes gives nonvanishing interference effects with the dominant photon-exchange amplitudes, and hence the major contribution from the Z_β boson at low energies is proportional to $\sin\beta$. One easily finds that this interference is destructive for R_{ll} whereas it is constructive for R . It is this downward shift of R_{ll} and the upward shift of R by the Z_β boson contribution that is responsible for the lowering of the overall χ^2 . These qualitative features are unchanged by the introduction of a small Z- Z_β mixing θ_E .

The data as well as the fit are given in Fig. 2. The solid curves (dotted curves) are predictions of the standard model with $\sin^2\theta_W=0.229$ and $M_Z=91.9$ GeV (89.0

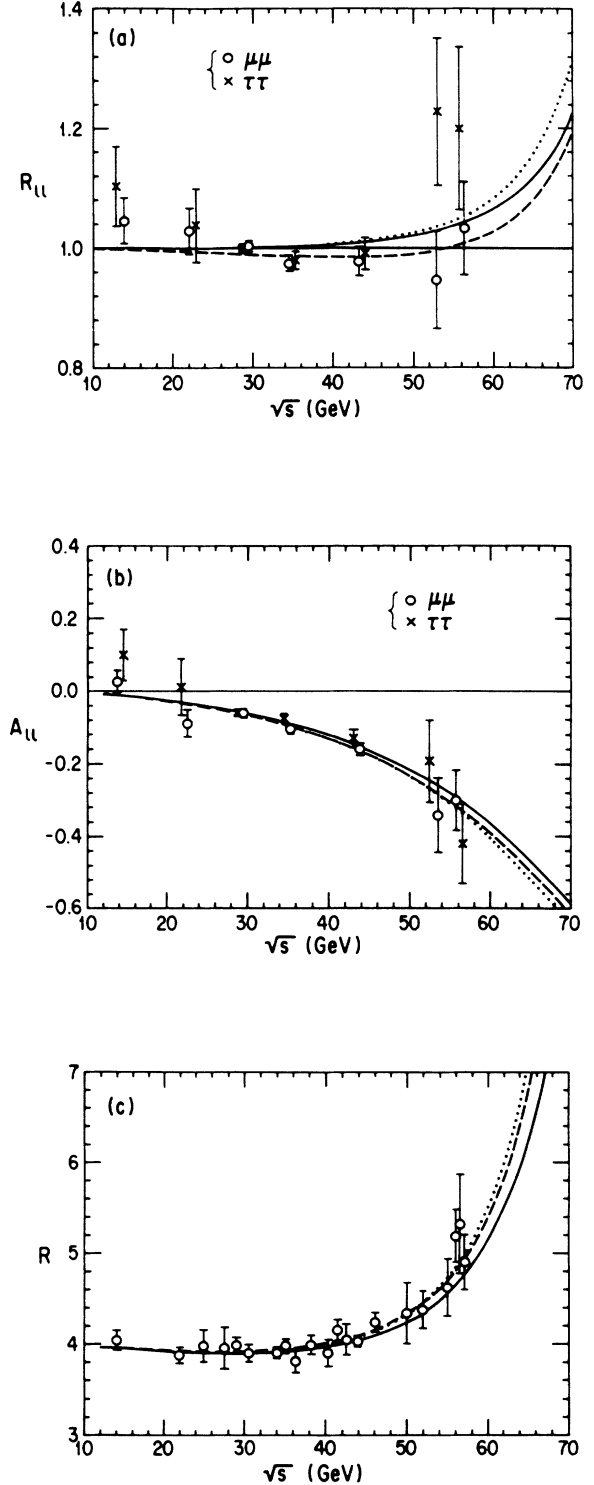


FIG. 2. (a) $R_{\mu\mu}$ and $R_{\tau\tau}$ data, (b) $A_{\mu\mu}$ and $A_{\tau\tau}$ data, and (c) R data as well as the fits are given as functions of \sqrt{s} . The solid curve (dotted curve) is the prediction of the standard model with $\sin^2\theta_W=0.229$ and $M_Z=91.9$ GeV (89.0 GeV). The dashed line is the prediction of the Z_χ model with $\sin^2\theta_W=0.229$, $M_1=91.6$ GeV, $M_2=192$ GeV, and $\theta_E=0.05$ rad. For display purposes, data from various experiments are combined by adding the statistical and systematic errors in quadrature.

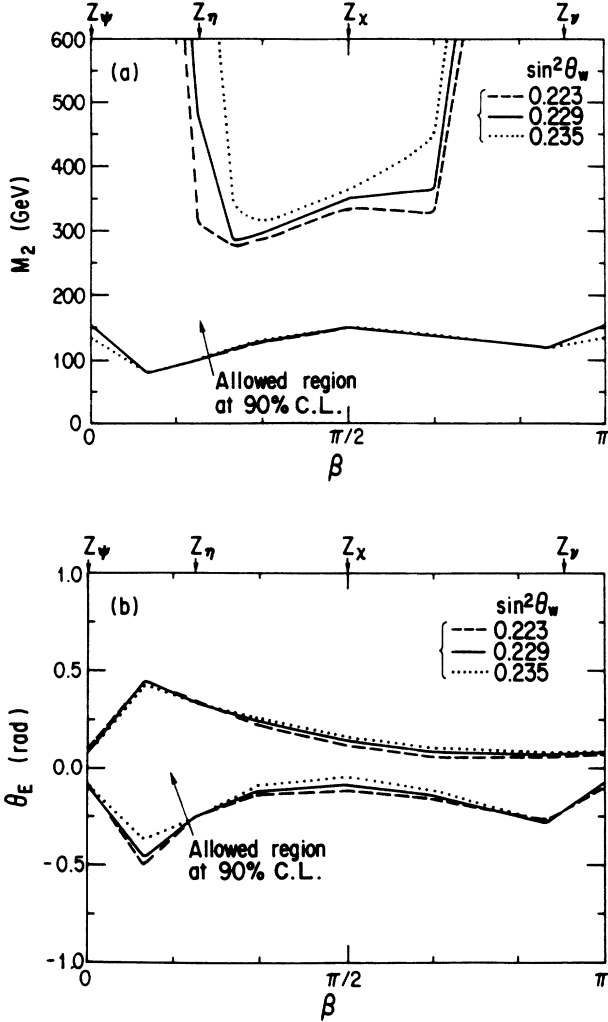


FIG. 3. Allowed regions for M_2 and θ_E at 90% C.L. ($\Delta\chi^2=2.71$) are plotted as functions of β , for the Z_β model. The limits are obtained for three values of $\sin^2\theta_W$: 0.223 (dashed lines), 0.229 (solid lines), and 0.235 (dotted lines).

GeV). The dashed lines give predictions of the Z_χ model with $M_2=192$ GeV and $\theta_E=0.05$ rad. The corresponding M_1 value is 91.6 GeV. It is noted that the average value of R_{ll} (for $l=\mu,\tau$) in the range $\sqrt{s}=30-50$ GeV is lower than 1 (0.98 ± 0.01). Since the vector coupling of charged leptons to the standard Z is nearly zero, it is hard for the standard model to give a good fit to the R_{ll}

data unless the value for $\sin^2\theta_W$ deviates significantly from $1/4$, as can be seen from the unconstrained fit in Table III. The R data is also slightly higher than the standard-model prediction. Figures 1 and 2 show that it is essential for Z_2^0 to have an appreciable vector coupling to charged leptons and down-type quarks in order to fit all e^+e^- data consistently. Such a feature, along with the behavior of $R_{\mu\mu}$ data, has been pointed out by Amaldi *et al.*² It is notable that the most recent publications from PETRA experiments are consistent with the trend observed in the older PETRA data of slightly lower R_{ll} . The TRISTAN data added a new feature of slightly higher R . These features are naturally expected in the class of E_6 -based extra Z models (Z_β) with large $\sin\beta$.

The allowed region for M_2 and θ_E at 90% C.L. ($\Delta\chi^2=2.71$) are plotted as functions of β in Fig. 3 for three values of $\sin^2\theta_W$; 0.223 (dashed line), 0.229 (solid line), and 0.235 (dotted line). From this figure, we find that there appears the 90%-C.L. upper mass limits for M_2 at 300–400 GeV range for models with $\pi/3 < \beta < 2\pi/3$. The upper limits are insensitive to $\sin^2\theta_W$ values for Z_χ , but those for Z_η are sensitive to $\sin^2\theta_W$. There are no upper limits of M_2 for Z_ψ and Z_ν . From Fig. 3(b), we observe that the mixing angle θ_E is generally small, except in the vicinity of $\beta\sim 0.3$.

Finally, we study three particular models Z_χ , Z_η , and Z_ψ in more details. As already noted, Z_χ gives a best fit, while Z_η is marginal. The other two models, Z_ψ and Z_ν , do not improve the fit significantly. Since the results for Z_ν are similar to those for Z_ψ , as can be seen from Figs. 3(a) and 3(b), we list only Z_ψ results as a reference. Details of the fit for Z_χ are summarized in Table IV, while Table V lists the results for Z_η and Z_ψ models. The errors given in the tables are calculated for $\Delta\chi^2=2.71$, which corresponds to a 90%-C.L. allowed range for each parameter. The allowed region in the M_2 - θ_E plane for the Z_χ model at 90% C.L. ($\Delta\chi^2=4.61$) is plotted in Fig. 4(a). In order to show the sensitivity of the present analysis to a particular value ($=0.229$) for $\sin^2\theta_W$, we also include the results with $\sin^2\theta_W=0.223$ and 0.235 in Tables IV and V. The results from the previous analysis³ are also shown in the figures. Contours obtained in Ref. 2 are consistent with those of Ref. 3. Our results are consistent with theirs.

In the case of Z_χ model, the relation $Y_H = -Y_{\bar{H}}$ $= -0.408$ holds and the Higgs constraint (9) reduces to

$$\tan\theta_E = \frac{2\lambda Y_H M_0^2}{M_2^2 - M_0^2} \sin\theta_W. \quad (21)$$

TABLE IV. Summary of fits for the Z_χ model. Errors given in the table are calculated for $\Delta\chi^2 = \chi^2 - \chi_{\min}^2 = 2.71$, which corresponds to the 90%-C.L. allowed region for each parameter.

	Lepton data	R data	All data	All data	All data
$\sin^2\theta_W$ (fixed)	0.229	0.229	0.223	0.229	0.235
M_1 (GeV)	91.9 ± 2.3	91.1 ± 2.6	91.7 ± 1.7	91.6 ± 1.7	$91.5^{+1.7}_{-1.8}$
M_2 (GeV)	192^{+351}_{-52}	$185^{+\infty}_{-48}$	191^{+145}_{-41}	192^{+166}_{-42}	195^{+168}_{-43}
θ_E (rad)	$0.04^{+0.10}_{-0.18}$	$0.09^{+0.13}_{-0.22}$	$0.01^{+0.11}_{-0.12}$	$0.05^{+0.09}_{-0.17}$	$0.08^{+0.08}_{-0.13}$
χ_{\min}^2/N_{DF}	88.9/142	56.5/72	145.8/219	145.9/219	146.0/219

TABLE V. Summary of fits for Z_η and Z_ψ models. All data are used. Errors given in the table are calculated for $\Delta\chi^2=2.71$.

	Z_η			Z_ψ		
$\sin^2\theta_W$ (fixed)	0.223	0.229	0.235	0.223	0.229	0.235
M_1 (GeV)	$91.3^{+1.6}_{-2.9}$	$91.3^{+1.6}_{-1.8}$	$91.2^{+1.7}_{-2.0}$	$90.5^{+2.1}_{-2.5}$	$90.5^{+2.2}_{-2.5}$	$90.5^{+2.2}_{-2.5}$
M_2 (GeV)	127^{+183}_{-26}	131^{+349}_{-31}	$143^{+\infty}_{-40}$	> 155	> 143	> 136
θ_E (rad)	$-0.01^{+0.36}_{-0.24}$	$-0.03^{+0.37}_{-0.22}$	$-0.08^{+0.42}_{-0.18}$	$-0.01^{+0.10}_{-0.06}$	$-0.02^{+0.10}_{-0.08}$	$-0.04^{+0.10}_{-0.06}$
χ^2_{\min}/N_{DF}	146.4/219	147.2/219	148.3/219	150.6/219	150.5/219	150.5/219

In this special case, the extra parameter is only M_2 for $\lambda=1$. The result of the fit for Z_χ boson with this constraint is given in Table VI. The significance of the Higgs constraint, which should be satisfied in all superstring-inspired models, is clearly seen in this simple example. The fit worsens by $\Delta\chi^2\sim 2.3$ since the line of this constraint is not around the minimum. Most importantly,

the mixing angle θ_E is not allowed to vanish for the Z_χ model. This leads to an important consequence for precision measurements on the Z resonance at the SLAC Linear Collider (SLC) and the CERN e^+e^- collider LEP. For other models, the effects of the Higgs-boson constraint are not so transparent, and we show it in Fig. 4(b) for the Z_η model. Regions under the dotted lines are allowed by the constraint. In this case, zero mixing is not excluded from the present data sample.

It is worth noting that our results are not very sensitive to the assumed $\sin^2\theta_W$ values. The region $0.223 < \sin^2\theta_W < 0.235$ covers both uncertainties coming from extra Z contribution to the low-energy NC experiments³ and the intrinsic uncertainty from the charm-quark mass dependence in the neutrino experiments.³³ Although the allowed region of M_1 is rather insensitive to the values for $\sin^2\theta_W$, there is a notable model dependence. The central value of M_1 is the smallest for the Z_ψ since the absence of interference with photon-exchange diagrams decouples direct Z_ψ contribution at low energies and its major effect is to make M_1 lighter through mixing. Since this does not improve the fit to R_{ll} data, the resulting χ^2 is largest for Z_ψ .

In order to see the sensitivity of our search, we tested the heavy “Z” boson, which the Particle Data Group calls a Z_1 boson,³⁰ whose couplings to quarks and leptons are the same as those of the standard Z boson. Assuming no mixing between Z and “ Z_1 ,” we obtain $M(“Z_1”) > 208$ GeV at the 90% C.L. with $\chi^2/N_{DF} = 149.9/220$. The fit does not improve at all since the vector coupling of “ Z_1 ” to charged leptons is nearly zero. Our result is comparable to the limits of about 180 GeV obtained under the same assumption by the UA1 and UA2 Collaborations.⁷

VI. CONCLUSIONS

In conclusion, we have tested the extra Z models expected in the E_6 grand unified theory by using the most recent e^+e^- annihilation data and the observed W/Z masses, and tried to explain somewhat high R ratios and low R_{ll} ($l=\mu, \tau$) values. We found that the data fit well for extra Z_β models with $\beta\sim\pi/2$ and its mass around 200 GeV. We obtain $150 < M_\chi < 363$ GeV, $M_\eta > 100$ GeV, and $M_\psi > 136$ GeV at 90% C.L. if $\sin^2\theta_W$ is in the region between 0.223 and 0.235 and $\Lambda_{\overline{MS}} = 0.15 \pm 0.03$ GeV. The upper mass limit for Z_χ disappears at the 2.7σ level since the fit gives the χ^2_{\min} value which is only $\Delta\chi^2=7.4$ below the standard model ($M_\chi = +\infty$, $\theta_E=0$).

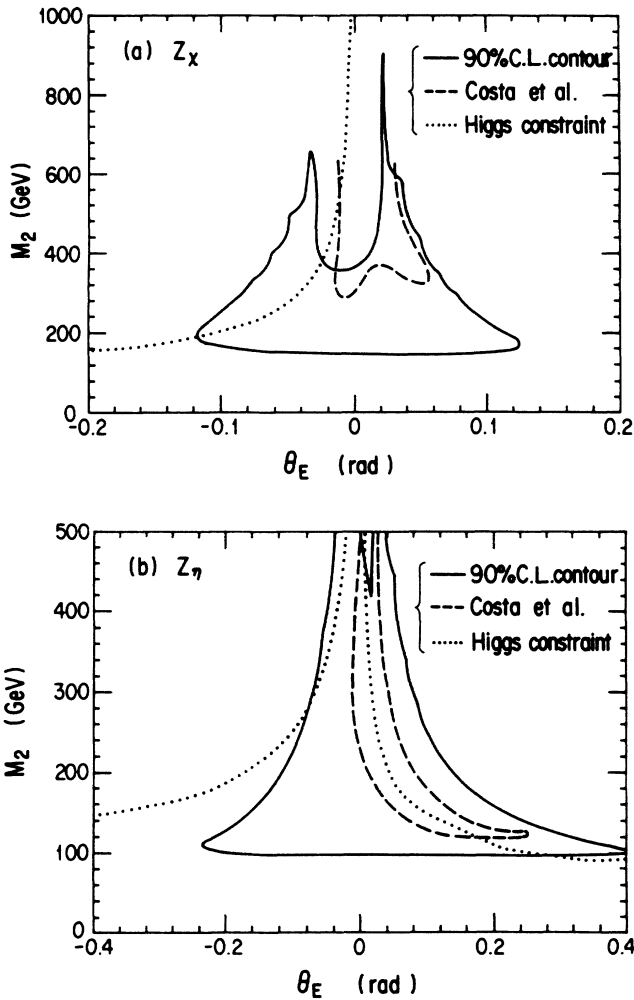


FIG. 4. Allowed regions in the M_2 and θ_E plane at 90% C.L. ($\Delta\chi^2=4.61$) are shown by solid lines for (a) Z_χ and (b) Z_η . Our results are consistent with those obtained by Amaldi *et al.* (Ref. 2) and by Costa *et al.* (Ref. 3). The latter results are plotted by dashed lines for comparison. Dotted lines show the Higgs constraint given in Eq. (21) for (a) Z_χ and that calculated from Eq. (9) for (b) Z_η .

TABLE VI. Fits for the Z_χ model with the Higgs constraint (21). Errors given in the table are calculated for $\Delta\chi^2=2.71$.

All data with Higgs constraint			
$\sin^2\theta_W$ (fixed)	0.223	0.229	0.235
M_2 (GeV)	236_{-54}^{+252}	246_{-58}^{+333}	256_{-65}^{+643}
θ_E (rad)	$-0.068_{-0.067}^{+0.055}$	$-0.063_{-0.065}^{+0.053}$	$-0.057_{-0.064}^{+0.053}$
$\chi_{\min}^2/N_{\text{DF}}$	148.1/220	148.2/220	150.7/220

From the lepton data only, we find $140 < M_\chi < 653$ GeV, $94 < M_\eta < 338$ GeV at 90% C.L., which are independent of $\Lambda_{\overline{\text{MS}}}$. These upper mass limits disappear at the 2σ level ($\Delta\chi^2=3.9$).

Our results are consistent with the lower limits obtained by the previous analysis.^{2,3,34} Although the significance of the upper limits for Z_β ($\beta\sim\pi/2$) is still marginal, we believe that such a feature in the published e^+e^- annihilation data is worth noting. The allowed region for the extra Z boson will become more restricted as TRISTAN experiments measure R_{ll} and A_{ll} more precisely and SLC and LEP produce accurate measurements of M_{Z_1} . The Fermilab Tevatron collider experiments will directly look for the production and decays of the extra Z bosons in the range 100–400 GeV.

After this work was completed, we received a new accurate measurement of M_{Z_1} from the Collider Detector at Fermilab (CDF) Collaboration,³⁵ which reads

$$M_{Z_1} = 90.9 \pm 0.4 \text{ GeV}, \quad (22)$$

after summing statistical and systematic errors in quadrature. we find that our global results are not affected much by the new datum with very small error and somewhat lower M_{Z_1} , which should soon be confirmed at SLC and LEP. For instance, by replacing (20b) by (22), we find for the Z_χ model $M_2 = 204_{-47}^{+205}$ GeV with

$\chi_{\min}^2/N_{\text{DF}} = 146.1/219$ as compared to $M_2 = 192_{-42}^{+166}$ GeV with $\chi_{\min}^2/N_{\text{DF}} = 145.9/219$ of Table IV. The new upper mass bound $M_2 < 409$ GeV disappears at the 2.3σ level since the standard-model fit is only $\Delta\chi^2=5.4$ worse than the Z_χ model fit. We note here that the standard-model fit improves by $\Delta\chi^2=1.9$ from $\chi_{\min}^2=153.4$ with $M_Z=91.9 \pm 1.8$ GeV to $\chi_{\min}^2=151.5$ with the new CDF value (22). For the Z_η model, the corresponding fit gives $M_2 = 127_{-27}^{+333}$ GeV with $\chi_{\min}^2/N_{\text{DF}} = 147.0/219$ as compared to $M_2 = 131_{-31}^{+349}$ GeV with $\chi_{\min}^2/N_{\text{DF}} = 147.2/219$ of Table IV. The new upper mass bound $M_2 < 460$ GeV disappears at the 2.1σ level ($\Delta\chi^2=4.5$). The allowed range for θ_E becomes somewhat smaller. The stability of the mass limits for the extra Z boson may have been expected from the preferred range of M_1 values listed in Tables IV and V which lie in the vicinity of 91 GeV not far from the new CDF data.

ACKNOWLEDGMENTS

The authors wish to thank Y. Shimizu for encouragement throughout this work. K.H. would like to thank D. Zeppenfeld for discussions and British Science and Engineering Research Council for financial support. The work of R.N. was supported in part by Research Institute of Yokohama College of Commerce.

- ¹S. L. Glashow, Nucl. Phys. **22**, 579 (1961); S. Weinberg, Phys. Rev. Lett. **19**, 1264 (1967); A. Salam, in *Elementary Particle Theory: Relativistic Groups and Analyticity (Nobel Symposium No. 8)*, edited by N. Svartholm (Almqvist and Wiksell, Stockholm, 1969), p. 367.
- ²U. Amaldi *et al.*, Phys. Rev. D **36**, 1385 (1987).
- ³G. Costa *et al.*, Nucl. Phys. **B297**, 244 (1988).
- ⁴UA1 Collaboration, G. Arnison *et al.*, Phys. Lett. **166B**, 484 (1986); UA2 Collaboration, R. Ansari *et al.*, Phys. Lett. B **186**, 440 (1987).
- ⁵V. Barger, N. G. Deshpande, and K. Whisnant, Phys. Rev. Lett. **56**, 30 (1986); Phys. Rev. D **35**, 1005 (1987).
- ⁶L. S. Durkin and P. Langacker, Phys. Lett. **166B**, 436 (1986); F. del Aguila, G. Blair, M. Daniel, and G. G. Ross, Nucl. Phys. **B283**, 50 (1987); T. Matsuoka, H. Mino, D. Suematsu, and S. Watanabe, Prog. Theor. Phys. **76**, 915 (1986).
- ⁷UA2 Collaboration, R. Ansari *et al.*, Phys. Lett. B **195**, 613 (1987); UA1 Collaboration, C. Albajar *et al.*, Z. Phys. C **44**, 15 (1989).
- ⁸AMY Collaboration, T. Mori *et al.*, Phys. Lett. B **218**, 499 (1989).

- ⁹R. Kajikawa, talk at the KEK Topical Conference on e^+e^- Physics, Tsukuba, 1989 (unpublished).
- ¹⁰F. Zwirner, Int. J. Mod. Phys. A **3**, 49 (1988), and references therein.
- ¹¹We note that the term ‘‘Higgs-boson constraint’’ was used in different contexts in the literature. Amaldi *et al.* (Ref. 2) used it in a weak sense for the tree-level constraint $\rho = M_W^2/(M_Z^2 \cos^2\theta_W) = 1$ which is automatically satisfied in models with only Higgs-doublet and Higgs-singlet fields, whereas Costa *et al.* (Ref. 3) required even stronger constraints than Eq. (9) by requiring either $0 < \bar{v}/v < 1$ or $0.2 < \bar{v}/v < 0.6$, which are motivated by the model of radiative electroweak symmetry breaking via the top-quark Yukawa coupling.
- ¹²D. London and J. L. Rosner, Phys. Rev. D **34**, 1530 (1986); V. Barger, N. G. Deshpande, J. L. Rosner, and K. Whisnant, *ibid.* **35**, 2893 (1987).
- ¹³Our notation closely follows that of Ref. 12. For comparison with other literature, one should note the following. The gauge fields (Z_ψ, Z_χ, Z_η) of Amaldi *et al.* (Ref. 2) are ($Z_\psi, -Z_\chi, -Z_\eta$) of our work, and their Z_β is our $Z_{\beta+\pi/2}$.

- The fields (Z_A, Z_B, Z_C) of the corresponding models in Costa *et al.* (Ref. 3) are (Z_η, Z_χ, Z_ν) of our work. Consequently, the signs of our mixing angle θ_E for Z_η and Z_χ models are opposite to those of Ref. 2. The overall scaling factor λ of Table II corresponds to $\sqrt{\lambda}$ of Ref. 2.
- ¹⁴J. Ellis, K. Enqvist, D. V. Nanopoulos, and F. Zwirner, *Mod. Phys. Lett.* **11**, 57 (1986); *Nucl. Phys.* **B276**, 14 (1986).
- ¹⁵L. E. Ibanez and J. Mas, *Nucl. Phys.* **B286**, 107 (1987); see also model (a) of Matsuoka *et al.* in Ref. 6.
- ¹⁶T. Yanagida, in *Proceedings of the Workshop on the Unified Theory and the Baryon Number in the Universe*, Tsukuba, Japan, 1979, edited by O. Sawada and A. Sugamoto (KEK, Tsukuba, 1979); M. Gell-Mann, P. Ramond, and R. Slansky, in *Supergravity*, edited by D. Freeman *et al.* (North-Holland, Amsterdam, 1979).
- ¹⁷J. Jersak, E. Laermann, and P. M. Zerwas, *Phys. Lett.* **98B**, 363 (1981); K. Hagiwara, M. Sakuda, and N. Terunuma, *Phys. Lett. B* **219**, 369 (1989).
- ¹⁸J. Jersak, E. Laermann, and P. M. Zerwas, *Phys. Rev. D* **25**, 1218 (1982); **36**, 310(E) (1987); S. Gsken, J. H. Khn, and P. M. Zerwas, *Phys. Lett.* **155B**, 185 (1985).
- ¹⁹S. G. Gorishny, A. L. Kataev, and S. A. Larin, *Phys. Lett. B* **212**, 238 (1988).
- ²⁰O. V. Tarasov, A. A. Vladimirov, and A. Yu. Zharkov, *Phys. Lett.* **93B**, 429 (1980).
- ²¹W. A. Bardeen, A. J. Buras, D. W. Duke, and T. Muta, *Phys. Rev. D* **18**, 3998 (1978).
- ²²S. Weinberg, *Phys. Lett.* **91B**, 51 (1980); L. Hall, *Nucl. Phys.* **B178**, 75 (1981); W. J. Marciano, *Phys. Rev. D* **29**, 580 (1984).
- ²³HRS Collaboration, M. Derrick *et al.*, *Phys. Rev. D* **31**, 2352 (1985); K. K. Gan *et al.*, *Phys. Lett.* **153B**, 116 (1985); S. Abachi *et al.*, *Phys. Rev. D* **40**, 902 (1989); Mark II Collaboration, M. Levi *et al.*, *Phys. Rev. Lett.* **51**, 1941 (1983); MAC Collaboration, W. W. Ash *et al.*, *ibid.* **55**, 1831 (1985); E. Fernandez *et al.*, *ibid.* **54**, 1620 (1985); CELLO Collaboration, H.-J. Behrend *et al.*, *Z. Phys. C* **14**, 283 (1982); *Phys. Lett. B* **191**, 209 (1987); *Phys. Lett.* **114B**, 282 (1982); *Phys. Lett. B* **222**, 163 (1989); Mark J Collaboration, B. Adeva *et al.*, *Phys. Rev. Lett.* **55**, 665 (1985); *Phys. Lett. B* **179**, 177 (1986); *Phys. Rev. D* **38**, 2665 (1989); PLUTO Collaboration, Ch. Berger *et al.*, *Z. Phys. C* **21**, 53 (1983); **28**, 1 (1985); JADE Collaboration, W. Bartel *et al.*, *ibid.* **30**, 371 (1986); TASSO Collaboration, M. Althoff *et al.*, *ibid.* **22**, 13 (1984); **26**, 521 (1985); W. Braunschweig *et al.*, *ibid.* **37**, 163 (1988); **43**, 549 (1989); TOPAZ Collaboration, I. Adachi *et al.*, *Phys. Lett. B* **208**, 319 (1988); AMY Collaboration, A. Bacala *et al.*, *ibid.* **218**, 112 (1989).
- ²⁴CELLO Collaboration, H.-J. Behrend *et al.*, *Phys. Lett. B* **183**, 400 (1987); VENUS Collaboration, H. Yoshida *et al.*, *ibid.* **198**, 570 (1987); TOPAZ Collaboration, I. Adachi *et al.*, *Phys. Rev. Lett.* **60**, 97 (1988); AMY Collaboration, T. Mori *et al.* (Ref. 8).
- ²⁵HRS Collaboration, P. Baringer *et al.*, *Phys. Lett. B* **206**, 551 (1988); JADE Collaboration, W. Bartel *et al.*, *Phys. Lett.* **146B**, 121 (1984); F. Ould-Saada *et al.*, *Z. Phys. C* **44**, 567 (1989); TASSO Collaboration, M. Althoff *et al.*, *Phys. Lett.* **126B**, 493 (1983); W. Braunschweig *et al.*, *Z. Phys. C* **44**, 365 (1989).
- ²⁶F. A. Berends and R. Kleiss, *Nucl. Phys.* **B177**, 237 (1981); F. A. Berends, R. Kleiss, and S. Jadach, *ibid.* **B202**, 63 (1983); *Comput. Phys. Commun.* **29**, 185 (1983).
- ²⁷M. Igarashi, N. Nakazawa, T. Shimada, and Y. Shimizu, *Nucl. Phys.* **B263**, 347 (1986).
- ²⁸J. Fujimoto and Y. Shimizu, *Mod. Phys. Lett. A* **3**, 581 (1988).
- ²⁹BCDMS Collaboration, A. C. Benvenuti *et al.*, *Phys. Lett. B* **195**, 97 (1987).
- ³⁰Particle Data Group, G. P. Yost *et al.*, *Phys. Lett. B* **204**, 1 (1988).
- ³¹W. Bernreuther and W. Wetzel, *Nucl. Phys.* **B197**, 228 (1982).
- ³²Three-loop effects both in the definition of $\Lambda_{\overline{MS}}$ (Refs. 20 and 30) and in the matching relation (Ref. 31) are found to be negligible as compared to the experimental error and the error caused by the uncertainty in m_b .
- ³³G. L. Fogli and D. Haidt, *Z. Phys. C* **40**, 379 (1988).
- ³⁴J. Ellis, P. Franzini, and F. Zwirner, *Phys. Lett. B* **202**, 417 (1988).
- ³⁵CDF Collaboration, F. Abe *et al.*, *Phys. Rev. Lett.* **63**, 720 (1989).